ChemPubSoc Europe

DOI: 10.1002/ejoc.201600835

EurJOC European Journal of Organic Chemistry

Full Paper

Glycomimetics

Diastereomeric Glycosyl Sulfoxides Display Different Recognition Features versus *E. coli* β-Galactosidase

Juan P. Colomer,[a] Beatriz Fernández de Toro,[b] F. Javier Cañada,[b] Francisco Corzana,[c] Jesús Jiménez Barbero,*[d,e,f] Ángeles Canales,*[g] and Oscar Varela*[a]

Abstract: The conformational analysis of the (*S*) and (*R*) diastereoisomers of benzyl 3-deoxy-4*S*-(β-D-galactopyranosyl)-4-thio-β-D-*threo*-pentopyranoside *S*-oxide (**1*S*** and **1*R***, respectively) has been performed by using NMR spectroscopy assisted by molecular modelling methods. The results point out that sulfoxide **1*S*** and **1*R*** display rather different conformational behaviors, **1*S*** being significantly more flexible than **1*R***. Both sulfoxides have shown to be competitive inhibitors of the β-galactosidase from *E.* coli, although with different potencies. The key structural features of the molecular recognition process have been characterized.

Introduction

Chemistry allows the design and synthesis of molecules resembling natural systems. Saccharide mimicry is an essential part of the development of sugar-based drugs and/or molecular probes. In fact, glycomimetics are sugar scaffolds bearing a relatively minimal modification that changes its properties while still resembling the carbohydrate molecule. Hence, modifications of the glycan moiety largely concentrate on the replacement of one or both the acetal oxygen atoms by another atom mainly a carbon, a nitrogen or a sulfur atom. In this context, in the field of glycomimetics, thiooligosaccharides have been largely recognized as important probes for the study of varied metabolic processes.[1] The replacement of the oxygen atom of the interglycosidic linkage by sulfur usually confers stability towards the hydrolysis by glycosidases[2] and, in many cases, thiooligosaccharides have been shown to act as inhibitors of such enzymes. Glycoside inhibitors are relevant for the understanding of many biological processes involved in signaling and recognition events. In recent years, the mechanism of action of the inhibitors has been studied, providing the basis for rational drug design.[3] In this regard, the development of novel thiodisaccharides can provide new avenues for the development of promising therapeutic agents for treatment of numerous diseases.[4]

Molecular recognition is at the heart of the biological response. Indeed, the interaction between a carbohydrate and a protein is the first step in the corresponding signaling process, and this event strongly depends on the structural features of the involved partners. In particular, the three-dimensional shape of the sugar is of paramount importance for the recognition event. Regarding carbohydrate-processing enzymes, such as glycosidase-mediated processes, it has been shown that during the catalytic events, a significant deformation of the conformation of the pyranose rings has been described for different enzyme–substrate complexes.[5] The observed distortion depends on the chemical nature of the sugar involved and on the particular enzyme, and takes place by passing from the typical $^4C_1$ chair to a half chair or sofa conformation.[6] This process has been deeply analyzed for the *Escherichia coli* β-galactosidase, a paradigmatic glycosidase, which has been extensively employed as a model enzyme.[7] The use of lactose mimetics has shown that this enzyme also distorts the ground-state conformation of the non-reducing (galactose) moiety of the glycosidic linkage, which is cleaved during the process.[8] The distortion permits the proper orientation of the aglycon, which is ready to depart from the catalytic site with minimum energy loss.[9]

In previous works, we have found experimental evidences of the existence of major conformational distortions in the molecular recognition process by the β-galactosidase from *E. coli* of thiodisaccharides containing a β-D-1-thiogalactose moiety *S*-

[a] *CIHIDECAR-CONICET-UBA, Department of Organic Chemistry, Exact and Natural Sciences Faculty, University of Buenos Aires*
Ciudad Universitaria, Pab. II, 1428 Buenos Aires, Argentina
E-mail: varela@qo.fcen.uba.ar
www.qo.fcen.uba.ar
[b] *Department of Chemical and Physical Biology, Biological Research Center, Spanish National Research Council (CIB-CSIC)*
Ramiro de Maeztu 9, 28040 Madrid, Spain
[c] *Department of Chemistry, Research Center of Chemistry Synthesis, University of La Rioja*
Madre de Dios 53, 26006 Logroño, Spain
[d] *CIC bioGUNE, Bizkaia Science and Technology Park, Building 801A, 48160 Derio, Spain*
E-mail: jjbarbero@cicbiogune.es
[e] *IKERBASQUE, Basque Foundation for Science, 48009 Bilbao, Spain*
[f] *Departament of Organic Chemistry II, Faculty of Science & Technology, University of the Basque Country, 48940 Leioa, Spain*
[g] *Department of Organic Chemistry I, Chemical Sciences Faculty, Complutense University, 28040 Madrid, Spain*
E-mail: ma.canales@quim.ucm.es
Supporting information for this article is available on the WWW under http://dx.doi.org/10.1002/ejoc.201600835.

(1→4)-bonded to a 3-deoxy-pentopyranose ring.[10] Thus, using a combination of NMR techniques and molecular modeling, a unique case of binding that involves a distorted geometry of the pentopyranose ring, instead of that of the galactose non-reducing end, was detected. We have herein investigated the behavior of a different family of glycomimetics, the novel thiodisaccharide *S*-oxides, acting as inhibitors of *E. coli* β-galactosidase. Interestingly, the rate of hydrolysis depended on the stereochemistry of the sulfoxide sulfur atom (see below).[11]

Thiodisaccharide sulfoxides are usually prepared by oxidation of the interglycosidic sulfur atom of thiodisaccharides. Sugar sulfoxides exhibit interesting biological activities; for example, the diastereomeric mixtures of sulfoxide derivatives of 3-deoxy-*S*-(1→4)-disaccharides inhibited the proliferation of selected tumor cell lines.[12] The diastereomeric mixtures of thiodisaccharide sulfoxides prepared in our laboratory could be separated in most of the cases. The absolute configuration of the sulfur stereocenter was assigned using NMR parameters, especially paying attention to the shielding/deshielding of the ^{1}H resonance signals caused by anisotropy of the S=O bond, and related effects.[11,13] In the present context, both the (S_S) and (R_S) diastereoisomers of benzyl 3-deoxy-4-S-(β-D-galactopyranosyl)-4-thio-β-D-*threo*-pentopyranoside *S*-oxides (**1*S*** and **1*R***, respectively) have shown to be competitive inhibitors of the β-galactosidase from *E. coli* with different potencies. Due to their chemical nature and the presence of a new stereocenter, sulfoxides **1*R*** and **1*S*** display different electronic and steric properties compared to those of the previously analyzed thiodisaccharides. In this work, the conformational analysis of these molecules has been performed by using NMR spectroscopy assisted by molecular modelling methods. Moreover, the key structural features of the molecular recognition process by *E. coli* β-galactosidase have been characterized using Saturation Transfer Difference (STD) experiments, again complemented by computational chemistry calculations.

Results and Discussion

The synthesis of thiodisaccharide sulfoxides **1*R*** and **1*S*** has been described previously.[11]

Conformational Analysis

First, ^{1}H-^{1}H coupling constants (*J*) were extracted from the 1D NMR spectra. As previously stated[11] for the analogous thioglycoside derivatives, the experimental *J* values of the aglycon ring for both **1*R*** and **1*S*** compounds were indicative of the existence of a conformational equilibrium between the $^1C_4$ and $^4C_1$ geometries (Figure 1).

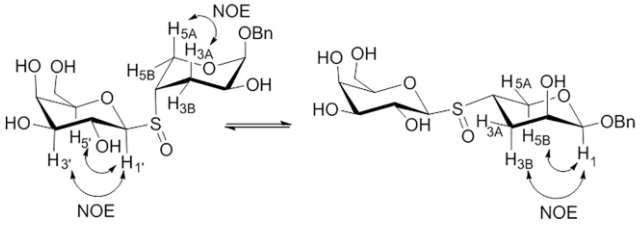

Figure 1. Conformational equilibrium of the aglyconic ring of **1*R*** and **1*S***.

The contribution of each chair was estimated from the comparison between the experimental *J* values and those calculated according to the generalized Karplus equation proposed by Altona, as implemented in the MSpin program[14] (Table 1). The data indicate that the $^1C_4$ conformation is the major form in both cases (75 %), also supported by the analysis of the intraresidue cross-peaks found in the 2D-NOESY spectra. The analogous analysis for the *galacto*-pyranose ring pointed out that the typical $^4C_1$ geometry is the exclusive conformation for this ring (Figure 2).

Table 1. Experimental and calculated coupling constant values [Hz] of the aglycon ring of **1*R*** and **1*S***.

^3J(H-H)	**1*R***			**1*S***		
	$J_{calcd.}$		$J_{exp.}$	$J_{calcd.}$		$J_{exp.}$
	$^1C_4$	$^4C_1$		$^1C_4$	$^4C_1$	
H_1-H_2	3.3	1.5	3.3	3.1	1.5	3.4
H_2-H_{3A}	11.1	3.3	10.7	11.2	3.2	11.2
H_2-H_{3B}	4.6	2.9	5.2	4.6	2.9	3.8
H_{3A}-H_4	4.8	3.8	3.8	5.1	3.9	4.8
H_{3B}-H_4	2	12.3	3.8	1.8	12.2	4.9
H_4-H_{5A}	3.1	4.6	3.8	3.7	4.4	2.8
H_4-H_{5B}	1.4	11.6	3.8	1.1	11.6	

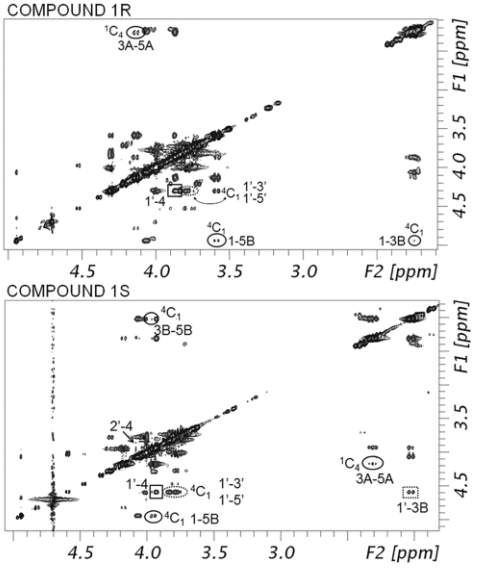

Figure 2. 2D-NOESY spectra (600 MHz, 600 ms mixing time, 310 K) recorded for **1*R*** and **1*S***. Key NOE cross-peaks for the $^1C_4$ and $^4C_1$ chairs are represented by circles, while those determining the glycosidic conformation are represented by squares. Dotted circles refer to the Gal ring, while complete circles represent both chairs of the aglycon ring. Complete square, dotted square, and line squares refer to the *syn*-Φ/*syn*-Ψ, *syn*-Φ/*anti*-Ψ and *anti*-Φ/*syn*-Ψ conformations, respectively.

The study of the conformation around the glycosidic sulfoxide linkage was then carried out. The corresponding torsion angles are defined as Φ = $H_{1'}$–$C_{1'}$–S–C_4 and Ψ = $C_{1'}$–S–C_4–H_4. The major contribution to the equilibrium conformation was elucidated by analyzing the key NOE cross-peaks. The observed NOE interaction between $H_{1'}$ and H_4, and the lack of NOE cross-peaks between $H_{2'}$–H_4 and $H_{1'}$–H_3, suggested the existence of an exclusive *syn*-Φ/*syn*-Ψ conformation for **1*R***.

Compound **1*S*** showed, similar to **1*R***, an intense NOE interaction between $H_{1'}$ and H_4, indicating that the *syn*-Φ/*syn*-Ψ conformation is the most populated geometry. However, two other minor conformers were also present in solution, the *syn*-Φ/*anti*-Ψ (as determined by the presence of an $H_{1'}$–H_{3B} NOE) and the *anti*-Φ/*syn*-Ψ (encoded by the weak $H_{2'}$–H_4 NOE) (Figure 2).

Ab initio Methods and Molecular Dynamics Simulations

Computational chemistry calculations using ab initio methods combined with molecular dynamics simulations were then performed.

The stability difference between the *syn*-Φ/*syn*-Ψ (the most populated conformation in both cases) and *anti*-Φ/*syn*-Ψ conformers for both compounds was first obtained.

According to the calculations, the energy difference between the different conformers is fairly different for the two compounds. For compound **1*S*** a 1.8 kcal/mol energy difference is found between the *syn*-Φ/*syn*-Ψ conformation and the *anti*-Φ/*syn*-Ψ conformer. In contrast, for **1*R***, the stability difference is significantly higher, ca. 3 kcal/mol. These data are in agreement with the presence in solution of the *anti*-Φ/*syn*-Ψ conformation only for **1*S***. This conformer is absent in **1*R***.

Molecular dynamics simulations for both compounds in the free state were then carried out. For **1*R***, the *syn*-Φ/*syn*-Ψ conformer was used as initial geometry, since this is the only one found in solution (see above). Indeed, it was observed that this conformation remained stable along all the trajectories. In contrast, **1*S*** showed conformational changes during the calculations, independently of the starting geometry. Transitions between the *syn*-Φ/*syn*-Ψ, *syn*-Φ/*anti*-Ψ and *anti*-Φ/*syn*-Ψ conformers were detected in all the calculations (Figure 3). These results again point out that sulfoxide **1*S*** is rather more flexible than **1*R***.

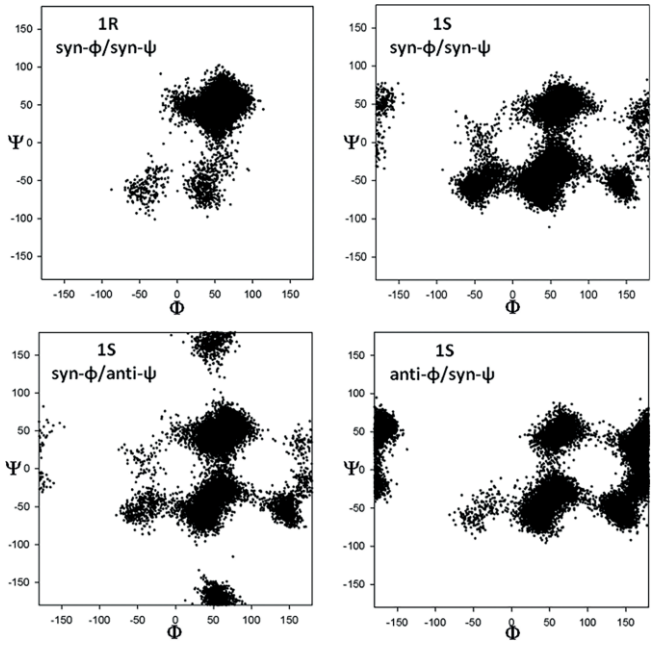

Figure 3. Plots of the evolution of the Φ/Ψ torsion angles around the sulfoxide linkage during the molecular simulations for **1*S*** and **1*R***. Torsion angles are defined as Φ = $H_{1'}$–$C_{1'}$–S–C_4 and Ψ = $C_{1'}$–S–C_4–H_4. Left top: *syn*-Φ/*syn*-Ψ conformation is maintained for **1*R***. Right top and bottom: *syn*-Φ/*syn*-Ψ is the most populated conformation for **1*S***.

The Bound State

The interaction between both ligands and the enzyme was then analyzed using NMR methods. Therefore, mixtures of both molecules **1*R*** and **1*S*** with *E. coli* β-galactosidase (300:1 molar ratio) were prepared to monitor the molecular recognition features.

Despite being a moderate inhibitor, the acquisition of ^{1}H NMR spectra at different times demonstrated the existence of a slow hydrolysis process of **1*R*** by the enzyme (Figure 4). Indeed, after 2.5 h of incubation with β-galactosidase (300:1 ligand/enzyme ratio), a small amount of galactose was detected. Galactose is the product of hydrolysis of **1*R***. Nevertheless, a significant amount of the sulfoxide **1*R*** remained unaffected after 20 h in presence of the enzyme. In contrast, when the analogous experiment was carried out for **1*S***, a very fast hydrolysis of this molecule under the same experimental conditions was evidenced (Figure 5).

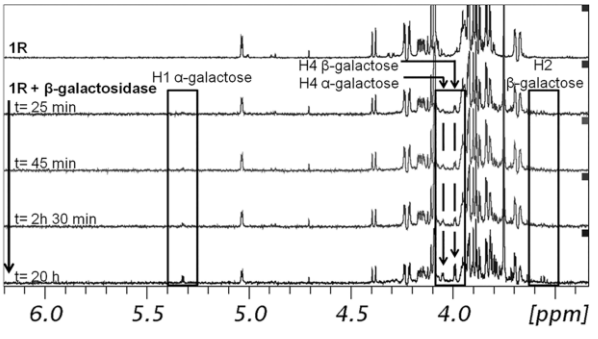

Figure 4. ^{1}H NMR spectra of **1*R***, free (top) and in the presence of *E. coli* β-galactosidase (300:1 molar ratio) at different times. The evolution of the newly formed α/β-galactose signals is highlighted.

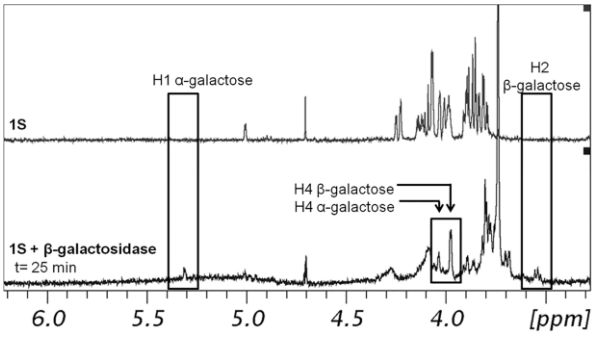

Figure 5. ^{1}H NMR spectra of **1*S***, free (top) and in the presence of *E. coli* β-galactosidase (300:1 molar ratio) after 25 min. The presence of the newly formed α/β-galactose signals is highlighted.

The slow hydrolysis observed for **1*R*** permitted to address key structural features of the molecular recognition process using ligand-based STD NMR molecular recognition experiments. The observed STD signals for **1*R*** in the presence of β-galactosidase pointed out that the protons with the highest STD intensities belong to the galactose unit. Indeed, the highest STD intensity corresponds to Gal H_2, H_3, and H_4 (Figure 6). Very minor STD peaks were observed for the aglycon.

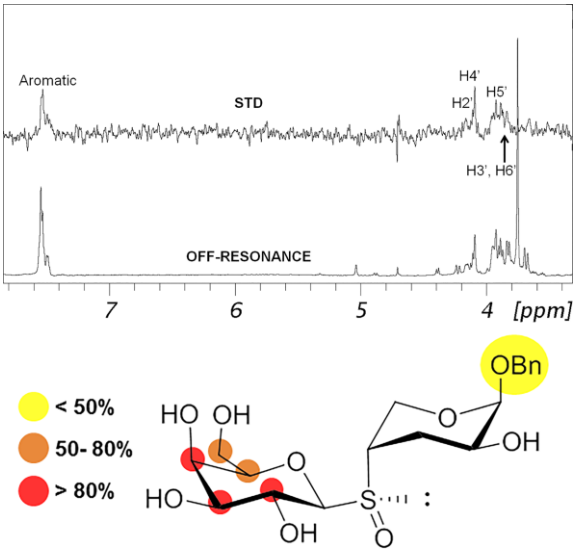

Figure 6. Top: STD experiment of **1*R***. The experiment (600 MHz) was performed with a 300:1 ligand/enzyme molar ratio in deuterated phosphate buffer (PBS) (20 mM, pH 7.2) at 300 K, with 1 mM $MgCl_2$. Off-resonance and on-resonance frequencies of 100 ppm and –1 ppm were applied, respectively. Bottom: Schematic representation of the observed STD percentages for **1*R***. Highest STD intensity protons belong to the Gal unit.

As mentioned above, the hydrolysis of **1*S*** was very fast. In order to obtain an overall picture of the hydrolysis process, the products obtained upon enzymatic hydrolysis of **1*S*** were analyzed.

D-Galactose and the aglycon ring are expected to be released when the hydrolysis takes place. However, the formation of an insoluble material was observed during the hydrolysis reaction, which was attributed to the benzyl pentopyranoside released, because of the low polarity of this moiety. Therefore, to investigate the outcome of this fragment, the solid material was isolated by centrifugation and subjected to acetylation in order to facilitate the chromatographic purification.

Two fractions were obtained whose main component was identified by HRMS (ESI). Thus, the less polar compound displayed an *m/z* value for the molecular ion, which was coincident with that of the disulfide **3b** (Scheme 1), while the $[M + H]^+$ ion of the more polar product was in agreement with that of the thiosulfinate **4b**.

The formation of these products can be justified if the hydrolysis of **1*S*** by the β-galactosidase produces the sulfenic acid **2** as a reactive intermediate. Sulfenic acids are assumed to

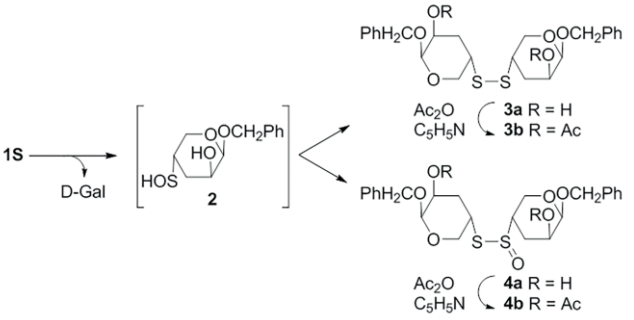

Scheme 1. Enzymatic reaction of sulfoxide **1*S*** by *E. coli* β-galactosidase: formation of products **3a** and **4a**. After acetylation, the respective compounds **3b** and **4b** were obtained.

be transient species in the oxidation of thiols to disulfides and sulfinic acids,[15] and may also be generated by chemical hydrolysis of glycosyl sulfoxides[16] or by enzymatic degradation of sulfoxides.[17] Due to their instability, sulfenic acids undergo several redox processes that are of great importance in biological events, and these reactions lead to varied products (including disulfides like **3a**). Indeed, when garlic or onions are cut, the naturally formed sulfenic acids are converted into different molecules, including the thiosulfinate as the self-condensation product.[17] Therefore, a similar conversion of **2** into **4a** can be expected.

It has been described previously that the high-energy *anti*-Φ/*syn*-Ψ conformer of C- and S-glycomimetics is recognized by *E. coli* β-galactosidase through a conformational selection process.[8b,10]

3D models of **1*S*** and **1*R*** in the binding site of the enzyme were obtained. The template employed to build these models was the X-ray structure of *E. coli* β-galactosidase in complex with galactose (PDB 1JZ7). The binding mode obtained by docking the *anti*-Φ/*syn*-Ψ conformers for both **1*S*** and **1*R*** in the binding site satisfactorily explains the hydrolysis process. The amino acid responsible for the nucleophilic attack, Glu^{537}, is fairly close to the anomeric position. Moreover, the hydroxy group at C_2 of the galactose residue, which is involved in the recruitment of the amino acid mentioned above, displays the proper orientation for the hydrolysis process.[18] In addition, the hydroxy group of Glu^{461}, which acts as the proton donor in the enzymatic process,[3c] is oriented towards the sulfoxide group, close to the oxygen atom (Figure 7). This disposition could favor the start of the hydrolysis reaction by protonation of the oxygen atom of the sulfoxide, according to the mechanism that involves the formation of a sulfenic acid intermediate, as described above.

However, the occurrence of this *anti*-Φ/*syn*-Ψ geometry is different for both isomers. According to the NMR spectroscopic data, this conformer is only found in solution for **1*S***.

Moreover, the comparison of the docked *anti*-Φ/*syn*-Ψ and *syn*-Φ/*syn*-Ψ conformers for both compounds in the binding site points out that only the *anti*-Φ/*syn*-Ψ conformation properly fits and displays the preferential geometry of the aglycon to behave as leaving group (Figure 8). In contrast, the *syn*-Φ/*syn*-Ψ conformation presents heavy steric clashes with the sur-

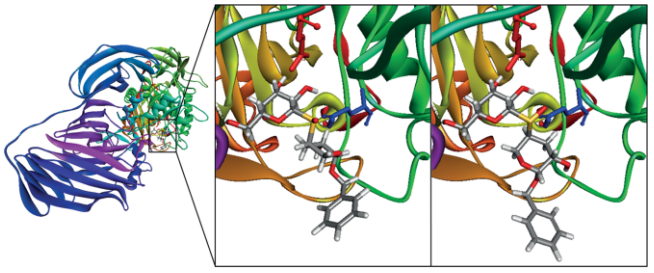

Figure 7. Representation of the complex of one of the four monomer domains of *E. coli* β-galactosidase docked with the *anti*-Φ/*syn*-Ψ conformer of **1*S*** (left) and **1*R*** (right). The orientation of the hydroxy group of the proton donor Glu^{461} (blue) towards the oxygen atom of the sulfoxide group, in addition to the disposition of Glu^{537} (red), confers the proper orientation for the initial hydrolysis process in both cases.

rounding amino acid residues (Figure S1). Therefore, the occurrence of the hydrolysis process in both cases, but preferentially in the **1*S*** isomer, can be satisfactorily explained.

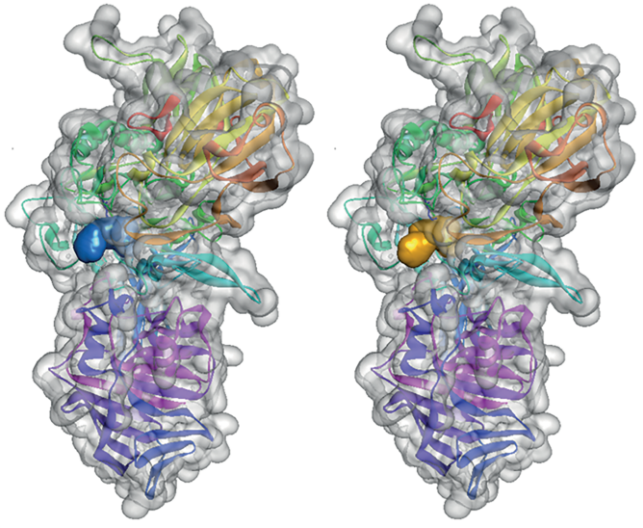

Figure 8. Surface representation of *E. coli* β-galactosidase in the complex with the *anti*-Φ/*syn*-Ψ conformer of **1*S*** (in blue, left) and **1*R*** (in orange, right). The proper orientation of the aglycon acting as leaving group is observed.

Conclusions

The conformational properties of a sulfoxide glycomimetic have been characterized in this work. Interestingly, the **1*R*** and **1*S*** stereoisomers display rather different conformational behaviors, as deduced from the NMR/molecular modeling analysis, although both act as moderate *E. coli* β-galactosidase inhibitors. Their inhibition potency depends on the stereochemistry at the sulfur atom. Despite their inhibition activity, both molecules are hydrolyzed by the enzyme, although at very different rates. The two molecules display different flexibilities, especially at the glycosidic linkage torsions, and are efficiently recognized by the enzyme.

The high flexibility of **1*S*** plays an important role in the molecular recognition process, and a conformational selection process takes place. The *anti*-Φ/*syn*-Ψ conformer is only present for **1*S***, while it is not observed for the **1*R*** analogue. The combination of NMR experimental data with modeling procedures permits to explain the observed different rates of hydrolysis.

Experimental Section

Enzymatic Assays and Identification of the Products of the Hydrolysis of 1*S*: The enzymatic hydrolysis of **1*S*** by the *E. coli* β-galactosidase was conducted as described previously.[11] After the enzymatic reaction, the formation of an insoluble material in the aqueous medium was observed. The solid was isolated by centrifugation and washed with water (5 mL). The aqueous solution and washing liquids were collected and monitored by NMR spectroscopy, revealing the presence of D-galactose. The residue of centrifugation was dried in vacuo and dissolved in $CDCl_3$ for NMR analysis. Once the spectra were recorded, the sample was acetylated with acetic anhydride (0.5 mL) and pyridine (0.5 mL) at room temp. for 16 h. The usual workup led to a product that showed by TLC (hexane/EtOAc, 1:1) two main spots with R_f = 0.70 and 0.40. Both components were separated by column chromatography using mixtures of increasing polarity of hexane/EtOAc (19:1 → 2:1). As the masses isolated were insufficient for NMR analysis, the structures of the main components were determined by HRMS (ESI). In the fraction with R_f = 0.70 was identified the disulfide **3b** (calcd. for $C_{28}H_{34}NaO_8S_2$ $[M + Na]^+$ 585.1587; found 585.1588). In the next fraction (R_f = 0.40) was identified the thiosulfinate **4b** (calcd. for $C_{28}H_{34}NaO_9S_2$ $[M + Na]^+$ 601.1536, found 601.1521).

Molecular Mechanics Calculations: A coordinate scan was performed by using Macromodel,[19] implemented in the Maestro suite of programs. MM3* force field was used to obtain different conformations in order to select those who agree with the NMR spectroscopic data. The calculation method used the PRCG protocol by employing an energy-minimization process. Full geometry optimization for the MM3* structures was performed with the Gaussian 03 program,[20] using the HF/6-31+G(d) basis set.[21]

Molecular Dynamics Simulations: 3 ns MD simulations of the compounds in the free state were performed with Amber 12[22] (ff99SB and GAFF force fields), in explicit TIP3P water at 298 K.

Docking Procedure: 3D models of **1*S*** and **1*R*** in the binding site of the enzyme were built by using Macromodel.[19] The structure of *E. coli* β-galactosidase in complex with galactose (PDB 1JZ7) was used as starting model. The galactose residue of both molecules were superimposed, and the resulting structures were refined by energy minimization with the AMBER force field as implemented in Macromodel; several steps of the Polak–Ribière conjugate gradient (PRCG) were used until the energy gradient become smaller than 0.05 kJ/mol/Å.

NMR Spectroscopy: NMR experiments were acquired at 310 K, using a Bruker AVANCE 600 MHz spectrometer equipped with a cryogenic probe. The concentration employed in the free-ligand experiments was 5 mM for both compounds. 1D ^1H NMR spectra, TOCSY (70 ms mixing time), NOESY (600 ms mixing time) and ^1H-^{13}C HSQC experiments were acquired, in order to assign all NMR signals. For 1D ^1H, TOCSY, NOESY and ^1H-^{13}C HSQC, the zgesp, dipsi2esgpph, noesyesgpph and hsqcedetgp sequences were employed. STD-NMR experiments (std2 sequence) were performed with a 300:1 ligand/enzyme molar ratio. An off-resonance frequency of 100 ppm and an on-resonance frequency of –1 ppm were applied, with 2 s of saturation time. Enzyme samples were recorded in sodium phosphate buffer (20 mM, pH 7.2) with 1 mM $MgCl_2$.

Acknowledgments

We thank the Spanish Ministerio de Economia y Competitividad (MINECO) for financial support (grants CTQ2012-32025, CTQ2015-64597-C2-1P, and CTQ2015-64597-C2-2P).

Keywords: Glycomimetics · Molecular recognition · Glycosidases · Conformation analysis

[1] a) H. Driguez, in *Glycoscience Synthesis of Substrate Analogs and Mimetics* (Eds.: H. Driguez, J. Thiem), Springer, Berlin–Heidelberg, **1998**, pp. 85–116; b) H. Driguez, *ChemBioChem* **2001**, *2*, 311–318.

[2] a) G. E. Ritchie, B. E. Moffatt, R. B. Sim, B. P. Morgan, R. A. Dwek, P. M. Rudd, *Chem. Rev.* **2002**, *102*, 305–320; b) M. R. Wormald, A. J. Petrescu, Y.-L. Pao, A. Glithero, T. Elliott, R. A. Dwek, *Chem. Rev.* **2002**, *102*, 371–386; c) H. Yuasa, C. Saotome, O. Kanie, *Trends Glycosci. Glycotechnol.* **2002**, *14*, 231–251; d) X. Wen, Y. Yuan, D. A. Kuntz, D. R. Rose, B. M. Pinto, *Biochemistry* **2005**, *44*, 6729–6737.

[3] a) B. Henrissat, A. Bairoch, *Biochem. J.* **1993**, *293*, 781–788; b) R. H. Jacobson, X. J. Zhang, R. F. DuBose, B. W. Matthews, *Nature* **1994**, *369*, 761–766; c) D. H. Juers, T. D. Heightman, A. Vasella, J. D. McCarter, L. Mackenzie, S. G. Withers, B. W. Matthews, *Biochemistry* **2001**, *40*, 14781–14794; d) M. L. Dugdale, M. L. Vance, R. W. Wheatley, M. R. Driedger, A. Nibber, A. Tran, R. E. Huber, *Biochem. Cell Biol.* **2010**, *88*, 969–979.

[4] a) Z. J. Witczak, *Curr. Med. Chem.* **1999**, *6*, 165–178; b) Z. J. Witczak, J. M. Culhane, *Appl. Microbiol. Biotechnol.* **2005**, *69*, 237–244; c) Z. J. Witczak, *Phosphorus Sulfur Silicon Relat. Elem.* **2013**, *188*, 413–417.

[5] a) X. Biarnés, A. Ardèvol, A. Planas, C. Rovira, A. Laio, M. Parrinello, *J. Am. Chem. Soc.* **2007**, *129*, 10686–10693; b) T. M. Gloster, G. J. Davies, *Org. Biomol. Chem.* **2010**, *8*, 305–320; c) A. Lammerts van Bueren, A. Ardèvol, J. Fayers-Kerr, B. Luo, Y. Zhang, M. Sollogoub, Y. Blériot, C. Rovira, G. J. Davies, *J. Am. Chem. Soc.* **2010**, *132*, 1804–1806; d) A. Martin, A. Arda, J. Désiré, A. Martin Mingot, N. Probst, P. Sinaÿ, J. Jiménez Barbero, S. Thibaudeau, Y. Blériot, *Nat. Chem.* **2016**, *8*, 186–191.

[6] A. T. Hadfield, D. J. Harvey, D. B. Archer, D. A. MacKenzie, D. J. Jeenes, S. E. Radford, G. Lowe, C. M. Dobson, L. N. Johnson, *J. Mol. Biol.* **1994**, *243*, 856–872.

[7] a) J. Pabba, A. Vasella, *Helv. Chim. Acta* **2006**, *89*, 2006–2019; b) B. P. Rempel, S. G. Withers, *Glycobiology* **2008**, *18*, 570–586.

[8] a) J. F. Espinosa, E. Montero, A. Vian, J. L. García, H. Dietrich, R. R. Schmidt, M. Martín-Lomas, A. Imberty, F. J. Cañada, J. Jiménez-Barbero, *J. Am. Chem. Soc.* **1998**, *120*, 1309–1318; b) A. García-Herrero, E. Montero, J. L. Muñoz, J. F. Espinosa, A. Vián, J. L. García, J. L. Asensio, F. J. Cañada, J. Jiménez-Barbero, *J. Am. Chem. Soc.* **2002**, *124*, 4804–4810.

[9] A. Vasella, G. J. Davies, M. Böhm, *Curr. Opin. Chem. Biol.* **2002**, *6*, 619–629.

[10] L. Calle, V. Roldós, F. J. Cañada, M. L. Uhrig, A. J. Cagnoni, V. E. Manzano, O. Varela, J. Jiménez-Barbero, *Chem. Eur. J.* **2013**, *19*, 4262–4270.

[11] J. P. Colomer, M. Á. Canales Mayordomo, B. Fernández de Toro, J. Jiménez-Barbero, O. Varela, *Eur. J. Org. Chem.* **2015**, 1448–1455.

[12] Z. J. Witczak, P. Kaplon, P. M. Dey, *Carbohydr. Res.* **2003**, *338*, 11–18.

[13] J. P. Colomer, V. E. Manzano, O. Varela, *Eur. J. Org. Chem.* **2013**, 7343–7353.

[14] *MSpin*, version 8.1.0-11315, Mestrelab Research S.L., **2012**.

[15] a) J. L. Kice, in *Advances in Physical Organic Chemistry*, vol. 17 (Eds.: V. Gold, D. Bethell), Academic Press Inc., London, **1981**, pp. 65–181; b) F. A. Davis, L. A. Jenkins, R. L. Billmers, *J. Org. Chem.* **1986**, *51*, 1033–1040; c) K. Goto, M. Holler, R. Okazaki, *J. Am. Chem. Soc.* **1997**, *119*, 1460–1461.

[16] J. Gildersleeve, R. A. Pascal, D. Kahne, *J. Am. Chem. Soc.* **1998**, *120*, 5961–5969.

[17] a) E. Block, J. Z. Gillies, C. W. Gillies, A. A. Bazzi, D. Putman, L. K. Revelle, D. Wang, X. Zhang, *J. Am. Chem. Soc.* **1996**, *118*, 7492–7501; b) E. Block, *Garlic and Other Alliums: The Lore and The Science*, The Royal Society of Chemistry, Albany, New York, USA, **2010**.

[18] B. W. Matthews, *C. R. Biol.* **2005**, *328*, 549–556.

[19] *MacroModel*, version 10.0, Schrödinger, LLC, New York, NY, **2013**.

[20] M. J. Frisch, G. W. Trucks, H. B. Schlegel, G. E. Scuseria, M. A. Robb, J. R. Cheeseman, J. A. Montgomery Jr., T. Vreven, K. N. Kudin, J. C. Burant, J. M. Millam, S. S. Iyengar, J. Tomasi, V. Barone, B. Mennucci, M. Cossi, G. Scalmani, N. Rega, G. A. Petersson, H. Nakatsuji, M. Hada, M. Ehara, K. Toyota, R. Fukuda, J. Hasegawa, M. Ishida, T. Nakajima, Y. Honda, O. Kitao, H. Nakai, M. Klene, X. Li, J. E. Knox, H. P. Hratchian, J. B. Cross, V. Bakken, C. Adamo, J. Jaramillo, R. Gomperts, R. E. Stratmann, O. Yazyev, A. J. Austin, R. Cammi, C. Pomelli, J. W. Ochterski, P. Y. Ayala, K. Morokuma, G. A. Voth, P. Salvador, J. J. Dannenberg, V. G. Zakrzewski, S. Dapprich, A. D. Daniels, M. C. Strain, O. Farkas, D. K. Malick, A. D. Rabuck, K. Raghavachari, J. B. Foresman, J. V. Ortiz, Q. Cui, A. G. Baboul, S. Clifford, J. Cioslowski, B. B. Stefanov, G. Liu, A. Liashenko, P. Piskorz, I. Komaromi, R. L. Martin, D. J. Fox, T. Keith, M. A. Al-Laham, C. Y. Peng, A. Nanayakkara, M. Challacombe, P. M. W. Gill, B. Johnson, W. Chen, M. W. Wong, C. Gonzalez, J. A. Pople, *Gaussian* 03, revision E.01, Gaussian, Inc., Wallingford, CT, **2004**.

[21] G. I. Csonka, *THEOCHEM* **2002**, *584*, 1–4.

[22] T. A. D. D. A. Case, T. E. Cheatham, III, C. L. Simmerling, J. Wang, R. E. Duke, R. Luo, R. C. Walker, W. Zhang, K. M. Merz, B. Roberts, S. Hayik, A. Roitberg, G. Seabra, A. W. G. J. Swails, I. Kolossváry, K. F. Wong, F. Paesani, J. Vanicek, R. M. Wolf, J. Liu, S. R. B. X. Wu, T. Steinbrecher, H. Gohlke, Q. Cai, X. Ye, J. Wang, M.-J. Hsieh, G. Cui, D. R. Roe, D. H. Mathews, M. G. Seetin, R. Salomon-Ferrer, C. Sagui, V. Babin, T. Luchko, S. Gusarov, A. Kovalenko, P. A. Kollman, *AMBER 12*, University of California, San Francisco, **2012**.

Received: July 8, 2016
Published Online: September 28, 2016